Synthesis and characterization of a functional polyhedral oligomeric silsesquioxane and its flame retardancy in epoxy resin

Kun Wu [a], Lei Song [a], Yuan Hu [a*], Hongdian Lu [a,b], Baljinder K. Kandola [c], Everson Kandare [c]

[a] State Key Laboratory of Fire Science, University of Science and Technology of China, 96 Jinzhai Road, Hefei, Anhui, 230027, PR China

[b] Department of Chemical and Materials Engineering, Key Laboratory of Powder and Energy Materials, Hefei University, Hefei, Anhui, 230022, PR China

[c] Centre for Materilas Research and Innovation, University of Bolton, Deane Road, Bolton, BL3 5AB, UK

Abstract

A functional polyhedral oligomeric silsesquioxane (NPOSS) with two epoxy ring groups was synthesized via the reaction between trisilanolisobutyl-POSS and triglycidyl isocyanurate, and then a halogen-free epoxy composite containing silicon/nitrogen was prepared. The results of microscale combustion calorimeter indicate that the presence of NPOSS (10% weight ratio) in epoxy resin (EP) can decrease its peak heat release rate by about 30%. The thermal oxidation and degradation behaviors of EP and EP/NPOSS composites were characterized by DSC, TG, FTIR-TG and dynamic FTIR. Scanning electron microscopy and X-ray photoelectron spectroscopy were used to explore the char residues of composites. The thermal degradation and flame retardant mechanism has been evaluated: NPOSS can retard the movement and scission of polymeric chains of EP and form a stable charred layer in the condensed phase to prevent the underlying materials from further combustion.

Keywords: Epoxy resin; POSS; TGIC; Flame retardancy; Thermal degradation; FTIR

*Corresponding author. Tel (Fax): + 86-551-3601664
E-mail address: yuanhu@ustc.edu.cn

1. Introduction

Epoxy resins (EP) are widely used as coatings and adhesives in modern industries because of their good chemical and electrical resistance, and attractive mechanical properties. Recently the research efforts on epoxy resins have been focused on improving their thermal stability, increasing glass transition temperatures and enhancing flame retardancy by satisfying halogen-free criterion [1]. To achieve above mentioned aims, it is reported that epoxy resins can be modified with boron [2], phosphorus [3-6], silicone [7, 8], polyurethanes [9], melamine and melamine phenol-formaldehyde resin [10] and montmorillonite [11], etc. Among them, the incorporation of silicone is considered as a promising method owing to its enhanced properties over the base polymer and its environmental friendliness [12].

Polyhedral oligomeric silsesquioxanes (POSS) are nano-sized cage structures with 1-3 nm particle size which can be incorporated into polymers to improve their thermal and oxidation resistance and reduce flammability [13]. These compounds can be represented as $(RSiO_{3/2})n$, where R can be hydrogen or any alkyl, alkylene, aryl, arylene groups, or organo-functional derivatives, etc. Laine and coworkers have done excellent work regarding different kinds of POSS and their polymer hybrids [14-18].

Based on above literatures, it can be anticipated that the incorporation of POSS in EP may improve its thermal and flame retardant properties. In this work, a functional POSS (NPOSS) was synthesized by the reaction between trisilanolisobutyl-POSS (TPOSS) which contains a partial T8 cage with one corner Si atom missing and triglycidyl isocyanurate (TGIC). And then a halogen-free organic/inorganic epoxy composites containing silicon/nitrogen was prepared. The chemical structure of NPOSS was characterized by Fourier transform infrared spectra (FTIR) and ^{29}Si NMR. NPOSS contains two epoxy ring groups and can be incorporated into the polymeric chain of EP to improve its flame retardancy, thermal and oxidation resistance. This work focuses on the study of flame retardancy, thermal oxidation and degradation behaviors of EP and EP/NPOSS composites using microscale combustion calorimeter (MCC), thermogravimetry (TG), TG-FTIR,

dynamic FTIR and differential scanning calorimeter (DSC), respectively. The chemical components and morphology of the char residue of EP/NPOSS composites were investigated by scanning electron microscopy (SEM) and X-ray photoelectron spectroscopy (XPS). The thermal degradation and flame retardant mechanism of EP and EP/NPOSS have also been evaluated.

2. Experimental

2.1. Materials

Trisilanolisobutyl-POSS ($C_{28}H_{66}O_{12}Si_7$, molecular weight = 791.42 g/mol) was purchased from Hybrid Plastics Company. Trisilanolisobutyl-POSS (TPOSS) contains a partial T8 cage with one corner Si missing, leaving three Si-OH groups. Triglycidyl isocyanurate (TGIC) was generously supplied by Huangshan Jinfeng Industrial Co., Ltd., China. Diglycidyl ether of biphenol A (DGEBA, E-44, epoxy equivalent = 0.44 mol/100 g) was provided from Jiangsu Wuxi Resin Plant, China. M-phenylenediamine and Tin (II) chloride were obtained from Shanghai Chemical Reagent Corporation, China. 1, 4-dioxane was used as solvent and supplied by Shanghai Chemical Reagent Corporation, China.

2.2. Synthesis of the novel POSS (NPOSS)

NPOSS was prepared by the reacting trisilanolisobutyl-POSS (TPOSS) and triglycidyl isocyanurate (TGIC) with Tin (II) chloride ($SnCl_2$) as a catalyst. First, 5.000 g of TPOSS, 1.973 g of TGIC and 0.005 g of $SnCl_2$ were dissolved in 80 ml of 1, 4-dioxane in a three-necked flask. The temperature of the reaction mixture was raised to 100 ^oC and held at that temperature for 4 h. After removing the 1, 4-dioxane by partial pressure distillation, the functional POSS (NPOSS) containing two epoxy ring groups was obtained. The synthesis process is illustrated in scheme 1.

2.3. Preparation of EP and its composites

NPOSS was dispersed in DGEBA at a temperature of 60 ^oC, followed by the

addition of the curing agent (m-Phenylenediamine) at equivalent ratio (wt/wt: 11.88/100). The mixtures were cured at 80 ^{o}C for 2 hours and postcured at 150 ^{o}C for 2 hours in an oven to obtain cured specimens. The weight percentage of NPOSS in epoxy composite is 10 wt%. The reaction process and structure of EP/NPOSS composite are shown in Scheme 2.

2.4. Measurements

2.4.1. Fourier Transform Infrared Spectroscopy

Samples were mixed with KBr powders, and the mixture was pressed into a tablet. FTIR spectra were recorded using Fourier transform spectrometer (Nicolet 6700).

2.4.2. ^{29}Si NMR

^{29}Si NMR spectra were recorded with a Bruker AVANCE 300 NMR spectrameter with $CDCl_3$ as a solvent.

2.4.3. Differential Scanning Calorimeter

DSC measurements were performed on a Perkin-Elmer Diamond DSC differential scanning calorimeter. Samples of about 5-10mg crimp-sealed in aluminum pans were heated at a heating rate of 20 ^{o}C/min under nitrogen atmosphere.

2.4.4. Microscale Combustion Calorimeter

The heat release rate (HRR) and the total heat release (THR) were measured in a microscale combustion colorimeter (GOVMARK MCC-2) for studying the molecular-level fire behaviors of materials. About 5 mg samples were heated at a heating rate of 1 K/s in a nitrogen stream flowing at 80 cm^3/min. The volatile, anaerobic thermal degradation products in the nitrogen gas stream were mixed with a 20 cm^3/min stream of pure oxygen prior to entering a 900 ^{o}C combustion furnace.

2.4.5. Thermogravimetry

The samples were examined on a TGA-Q5000 apparatus (TA Company, USA) at a heating rate of 10 ^{o}C /min. The weight of all samples was kept within 3-5 mg in an open Al pan.

2.4.6. Thermogravimetry-Fourier Transform Infrared Spectroscopy

The TG-FTIR instrument consists of analyzer (TGA-Q5000, TA Company, USA)

coupled with Fourier transform spectrometer (Nicolet 6700) via a transfer line. The investigations were carried out at a heating rate of 10 ^{o}C/min under nitrogen atmosphere at a flow rate of 35.0 ml/min. In order to reduce the possibility of gases condensing along the transfer line, the temperature in the gas cell and transfer line were set to 230 ^{o}C.

2.4.7. Dynamic Fourier Transform Infrared Spectra

Real time FTIR spectra of EP/NPOSS were recorded using Nicolet MAGNA-IR 750 spectrophotometer equipped with a ventilated oven having a heating device. The temperature of the oven was raised at a heating rate of about 10 ^{o}C/ min. Samples were mixed with KBr powders, and the mixture was pressed into a tablet. Dynamic FTIR spectra were obtained in situ during the thermal degradation of the samples.

2.4.8. Scanning Electron Microscopy

The samples were sputter-coated with a conductive layer. Then the SEM micrographs of the char residue were obtained with a scanning electron microscope AMRAY1000B.

2.4.9. X-ray Photoelectron Spectroscopy Spectra

The XPS spectra of the char residue were recorded with a VG Escalab mark II spectrometer (VG Scientific Ltd, UK), using Al Ka excitation radiation (1253.6 eV).

3. Results and Discussion

3.1. FTIR and ^{29}Si NMR

Fig. 1 shows the FTIR spectra of TGIC, TPOSS and NPOSS. The Si-O- group can be detected in the range of 1050-1150 cm^{-1} [19]. The change of the shape of FTIR spectra for NPOSS demonstrated the occurrence of the reaction between Si-OH and epoxy ring. Moreover, the shift of peak at 3235 cm^{-1} (Si-O-H) further confirms the reaction.

^{29}Si NMR analysis (Fig. 2) also gives evidence to the formation of NPOSS. For TPOSS, three different peaks were found at -68.5, -67.2 and -58.9 ppm, respectively. However, there exist four peaks in the spectrum of NPOSS. The existence of T^4 at

58.1 ppm represent that the bond was formed between the Si-OH of TPOSS and the epoxy ring of TGIC.

3.2. Microscale Combustion Calorimeter

Microscale combustion calorimeter (MCC) is a new, rapid, lab scale test that uses thermal analysis methods to measure chemical properties related to fire. From just a few milligrams of specimen a wealth of information on material combustibility and fire hazard is obtained in minutes.

The curves of the heat release rate (HRR) of EP and EP/NPOSS composites are shown in Fig. 3. The HRR curve of neat EP shows a sharp peak. Associated data for EP are: peak HRR =553.5 w/g, Total heat release (THR) = 24.6 KJ/g. In the case of EP/NPOSS composites, incorporation of 10 wt% NPOSS into EP leads to occurrence of two overlapping peaks in its HRR curve. Associated data for EP/NPOSS are: first peak HRR =13.8, second peak HRR=368.8 w/g, THR = 24.7 KJ/g. Though the addition of NPOSS does not significantly change the THR, the peak HRR is sharply reduced. It can be concluded that the incorporation of NPOSS into the EP was beneficial for improving the flame retardancy of EP.

Fig. 4 shows the SEM photographs of the residual char of EP and EP/NPOSS at the end of MCC test. The residual char of EP presents a smooth and continual char layer on which are dispersed some folds. For EP/NPOSS, its residual char is very flat.

3.3. DSC study

Fig. 5 shows the DSC curves of EP and EP/NPOSS. No obvious exothermic/endothermic peaks are observed, and this confirmed the high conversion of the condensation reaction in the curing reaction [20]. The temperature at the baseline shift is read as Tg which is aroused by the movement of epoxy molecular chains. The Tg of EP/NPOSS (166 ^{o}C) is higher than that of pure resin (145 ^{o}C). Above phenomenon indicates that the NPOSS may restrict the movements of polymer chains of EP.

3.4. TG analysis

TG and DTG curves of TPOSS, TGIC, NPOSS, EP and EP/NPOSS in air atmosphere are presented in Fig. 6. The initial decomposition temperature can be considered as the temperature at which the weight loss was about 5%. [19] The onset degradation temperature of samples which was evaluated by the temperature of 5 wt% weight loss ($T_{-5\%}$), the mid-point temperature of the degradation ($T_{-50\%}$) and the solid residue left at 700 ^{o}C were obtained from the TG curve; the temperature of the maximum weight loss rate (T_{max}) of samples was obtained from the DTG curve. These data are shown in Table 1.

Fig. 6 shows that TPOSS starts to decompose at 188 ^{o}C. The thermal oxidative degradation process of TPOSS has only one stage and its corresponding T_{max} is 200 ^{o}C. The degradation occurs until 400 ^{o}C, leaving residual yield of 44.3%. The thermal oxidative degradation process of TGIC in air is mainly composed of three steps. Its initial decomposition temperature is about 196 ^{o}C. The residue weight for TGIC at the temperature of 700 ^{o}C is 1.1%.

In Fig. 6, the thermal oxidative degradation process of NPOSS is composed of three steps and their corresponding T_{max} is 192, 316 and 517 ^{o}C, respectively. NPOSS begins to lose weight at about 169 ^{o}C which is earlier compared with that of TGIC or TPOSS. This can be explained by the reaction between the TPOSS and TGIC. It is interesting that in the temperature range of 229-326 ^{o}C, the TG curves of NPOSS shifts to higher temperature compared with that of TGIC or TPOSS. The stable solid residue of NPOSS at 700 ^{o}C is 21.0%.

In regard to EP, its initial decomposition temperature is about 308 ^{o}C, and degrades almost completely below 640 ^{o}C. From Fig. 6, it can be seen that EP/NPOSS begins to lose weight earlier than EP due to the relative weak thermal stability of NPOSS at low temperature. However, beyond the temperature of 450 ^{o}C, EP/NPOSS is more stable than EP. EP/NPOSS leaves 1.8% residual char at 700 ^{o}C, which is higher than of EP. It can be drawn that the addition of NPOSS can improve the thermal stability and retard the thermal oxidative degradation of EP at high temperature.

3.5. TG-FTIR analysis of EP and EP/NPOSS

In this work, TG-FTIR was used to analyze the gas products during the thermal degradation process.

Fig. 7 shows the 3D TG-FTIR spectrum of gas phase in the thermal degradation of EP. In Fig. 6, peaks in the regions of around 3500–4000 cm^{-1}, 2000–2400 cm^{-1}, 1600–1800 cm^{-1}, 1250–1600 cm^{-1} and 1100-1200 cm^{-1} were noted. FTIR spectra of pyrolysis products of EP at different time are shown in Fig. 8. The main products of the thermal decomposition of EP are compounds containing –OH (such as H_2O, phenol; 3500-4000 cm^{-1}), CO_2 (2360 cm^{-1}), CO (2180, 2117 cm^{-1}), hydrocarbons (C–H stretching at 1249 and 1167 cm^{-1}), compounds containing carbonyl (1700-1800 cm^{-1}) and compounds containing aromatic ring (1370-1600 cm^{-1}), etc. [21-24] Associated with the analysis of Fig. 9, it can be draw that the pyrolysis products for EP at the beginning (from about 20.0 min) are mainly composed of H_2O and CO_2, etc. With the increase of temperature (above30.0 min), CO, hydrocarbons, compounds containing carbonyl and aromatic ring, etc. are released.

As shown in Fig. 10 and Fig. 11, the evolved gas analysis for EP/NPOSS exhibited characteristic bands of compounds containing –OH group (e.g. H_2O, phenol; 3500-4000 cm^{-1}), methyl-substituted compounds (CH_2/CH_3 stretching, 2860–2970 cm^{-1}), CO_2 (2360 cm^{-1}), CO (2180, 2117 cm^{-1}), compounds containing carbonyl (1700-1800 cm^{-1}), compounds containing aromatic ring (1340-1600 cm^{-1}), hydrocarbons (C–H stretching at 1261 and 1171 cm^{-1}), etc. Associated with the analysis of Fig.9, it can be draw that the pyrolysis products for EP/NPOSS at the beginning (from about 15.2 min) are mainly composed of compounds containing carbonyl and aromatic ring and hydrocarbons. With the increase of temperature (above about 31.2 min), methyl-substituted compounds, compounds containing carbonyl and aromatic ring, etc. are released.

From above results, it is noted that the main evolved gas products for EP are different from that of EP/NPOSS. The main evolved gas products of EP are composed of small molecule, such as CO_2 and CO, etc. In another aspect, EP/NPOSS releases

mainly methyl-substituted, carbonyl and aromatic ring which have higher molecular weight compared with that of EP gas products. The reason can be assumed that the presence of NPOSS with cage structure can retard the movement and destruction of the main chain of EP during its thermal degradation. So, EP is easily to be broken and release gas containing more little molecular fragments under heating compared with EP/NPOSS.

3.6. Thermal oxidative degradation of EP/NPOSS

Fig. 12 shows the dynamic FTIR spectra of EP/NPOSS. The details of the thermal oxidative behavior of EP/NPOSS can be revealed by the dynamic FTIR.

In Fig. 12, the main characteristic absorption bands show few changes in the temperature range from room temperature to 150 ^{o}C. The changes of C-H absorption of aliphatic groups can be used to evaluate the thermal stability of samples during thermal oxidative degradation. From Fig. 12，it is clear that the intensities of the bands at 2966 and 2870 cm^{-1} (CH_2 and CH_3 asymmetric and symmetric vibrations) and 1460 cm^{-1} (CH_2 and CH_3 deformation vibration) decrease gradually up until the pyrolysis temperature of 350 ^{o}C due to the thermal oxidative degradation of EP main chains [23, 25]. The weak bands at around 1400-1600, 1150-1300 cm^{-1} at 350 ^{o}C may be corresponding to polyaromatic substituted phenols. Moreover, the inducement of oxygen accelerates the formation of the crosslinked polyaromatic carbonaceous residue [26]. NPOSS can interfere with the free radical oxidative degradation process of EP. The isobutyl radical can capture the hydrogen radical and the silicon radical of NPOSS can capture the hydroxy radical (Scheme 3). As a result, NPOSS can play a role of radical trap via the consuming of highly reactive hydrogen and hydroxy radicals. It is interesting to find that between the range of 400 and 500 ^{o}C, the shape of spectra show few change. This may be attributed to the formation of stable structures containing Si-O- (1087 cm^{-1}) and phenyl (814 cm^{-1}) complexes [27].

It is proposed herein that the presence of NPOSS can capture the hydrogen and hydroxyl radical and form a stable charred layer in the condensed phase. The char becomes a better thermal insulating layer, prevents heat from reaching the remaining

polymer, and retard further thermal degradation of underlying materials. These results are in agreement with the data obtained from TG and MCC.

3.7. XPS analysis

The chemical components of the residual char for EP/NPOSS (heated in muffle furnace for 10 minutes at 600 ^{o}C) were investigated by XPS. The results of the XPS spectra are shown in Table 2.

The peak at 284.6 eV is attributed to C-H and C-C in aliphatic and aromatic species. The peak at 285.9 eV is characteristic of C-O (ether and/or hydroxyl group) [28]. Moreover, the peak at 288.5 eV can be assigned to C=O and/or C=N, respectively [29].

Two bands at 532.6 and 534.5 eV are observed from O_{1s} spectra. It is known that it is impossible to distinguish inorganic and organic oxygen because the O_{1s} band is structureless. The peak centred at 532.6 is assigned to C-O group. [30] The peak at 534.5 eV corresponds to Si-O group.

For N_{1s} spectra, the weak peaks around 400.7 eV are due to the nitrogen functionality in pyrrolic group. Bourbigot et al. reported that the peak corresponding to pyridinic group was referred as N-6 (six-membered ring). [30] The peak at 103.2 eV can be assigned to Si-O group in the residual char.

4. Conclusion

In this paper, NPOSS with a cage structure was incorporated into the network of epoxy resin (EP), increasing its flame retardancy and thermal stability at high temperature. During thermal degradation, EP is easily broken and release compounds containing small molecules, such as CO_2 and CO, etc. However, EP/NPOSS releases mainly methyl-substituted, carbonyl and aromatic ring compounds with higher molecular weight compared with that of EP. The presence of NPOSS with cage structure can retard the movement and scission of the main chain of EP during thermal degradation process. Moreover, the results of dynamic FTIR, XPS and SEM

show that NPOSS may capture the hydrogen and hydroxyl radical and form a stable charred layer in the condensed phase which would prevent the underlying materials from further destruction during combustion.

Acknowledgements

The financial support from the National 11th Five-year Program (2006BAK01B03、2006BAK06B06、2006BAK06B07) and China Postdoctoral Science Foundation (20080430101) is acknowledged.

References

[1] Y.L. Liu, Hsu CY, W.L. Wei, R.J. Jeng, Polymer 44 (2003) 5159.

[2] C. Martin, G. Lligadas, J.C. Ronda, M. Galia, V. Cadiz, J Polym Sci: Pol Chem. 44 (2006) 6332.

[3] J. Artner, M. Ciesielski, O. Walter, M. Doring, R.M. Perez, J.K.W. Sandler, V. Altstadt, B. Schartel, Macromol. Mater. Eng. 293 (2008) 503.

[4] C.H. Lin, T.Y. Hwang, Y.R. Taso, T.L. Lin, Macromol. Chem. Phys. 208 (2007) 2628.

[5] X.H. Zhang, F. Liu, S. Chen, G.R. Qi, J. Appl. Polym. Sci. 106 (2007) 2391.

[6] C.H. Lin, C.C. Feng, T.Y. Hwang, Eur. Polym. J. 43 (2007) 725.

[7] S.A. Kumar, Z. Denchev, M. Alagar, Eur. Polym. J. 42 (2006) 2419.

[8] Y.C. Chiu, F.Y. Liu, C.C.M. Ma, I.C. Chou, L. Riang, C.L. Chiang, J.C. Yang, Thermochim. Acta. 473 (2008) 7.

[9] C.S. Wu, Y.L. Liu, Y.S. Chiu, J. Appl. Polym. Sci. 85 (2002) 2254.

[10] J.Y. Shieh, C.S. Wang, Polymer 42 (2001) 7617.

[11] E. Kaya, M. Tanoglu, S. Okur, J. Appl. Polym. Sci. 109 (2008) 834.

[12] C.S. Wu, Y.L. Liu, Y.S. Chiu, Polymer 43 (2002) 4277.

[13] A. Fina, H.C.L. Abbenhuis, D. Tabuani, G. Camino, Polym. Degrad. Stab. 91 (2006) 2275.

[14] S.G. Kim, J. Choi, R. Tamaki, R.M. Laine, Polymer 46 (2005) 4514.

[15] J. Choi, A.F. Yee, R.M. Laine, Macromolecules 36 (2003) 5666.

[16] R. Tamaki, J. Choi, R.M. Laine, Chem. Mater. 15 (2003) 793.

[17] R.M. Laine, J. Choi, I. Lee, Adv. Mater. 13 (2001) 800.

[18] J. Choi, J. Harcup, A.F. Yee, Q. Zhu, R.M. Laine, J. Am. Chem. Soc. 123 (2001) 11420.

[19] T.L. Lu, G.Z. Liang, Y.L. Peng, T. Chen, J. Appl. Polym. Sci. 106 (2007) 4117.

[20] F. Rubio, J. Rubio, J.L. Oteo, Thermochim. Acta. 307 (1997) 51.

[21] U. Braun, B. Schartel, M.A. Fichera, C. Jager, Polym. Degrad. Stab. 92 (2007) 1528.

[22] R.R. Baker, S. Coburn, C. Liu, J. Tetteh, J. Anal. Appl. Pyrolysis. 74 (2005) 171.

[23] N.B. Colthup, L.H. Daly, S.E. Wiberley, “Introduction to Infrared and Raman Spectroscopy”, 2nd edition, Academic Press, Boston 1990.

[24] A.I. Balabanovich, A. Hornung, D. Merz, H. Seifert, Polym. Degrad. Stab. 85 (2004) 713.

[25] J.F. Xiao, Y. Hu, L. Yang, Y.B. Cai, L. Song, Z.Y. Chen, W.C. Fan, Polym. Degrad. Stab. 91 (2006) 2093.

[26] S.V. Levchik, E.D. Weil, Polym. Int. 54 (2005) 981.

[27] Y.Q. Zhao, D.A. Schiraldi, Polymer 46 (2005) 11640.

[28] S.W. Zhu, W.F. Shi, Polym. Degrad. Stab. 80 (2003) 217.

[29] Y. Nakayama, F. Soeda, A. Ishitani, Carbon 28 (1990) 21.

[30] S. Bourbigot, M. Le Bras, R. Delobel, L. Gengembre, Appl. Surf. Sci. 120 (1997)

Table 1 TG and DTG data of the samples

Sample code	$T_{-5\%}$ (^{o}C)	$T_{-50\%}$ (^{o}C)	T_{max} (^{o}C)	Solid residue (%) at 700 ^{o}C
TPOSS	188	320	200	44.3
TGIC	196	240	237	1.1
NPOSS	169	330	193	21.0
EP	308	399	352	0.2
EP/NPOSS	231	398	353	1.8

Table 2 XPS results of the residual char of EP/NPOSS

System	Peak binding energy (eV)	Area (%)
C 1s	284.6	28.26
C 1s	285.9	11.00
C 1s	288.5	5.33
O 1s	532.6	40.16
O 1s	534.5	4.59
N 1s	400.7	0.74
Si 2p	103.2	9.91

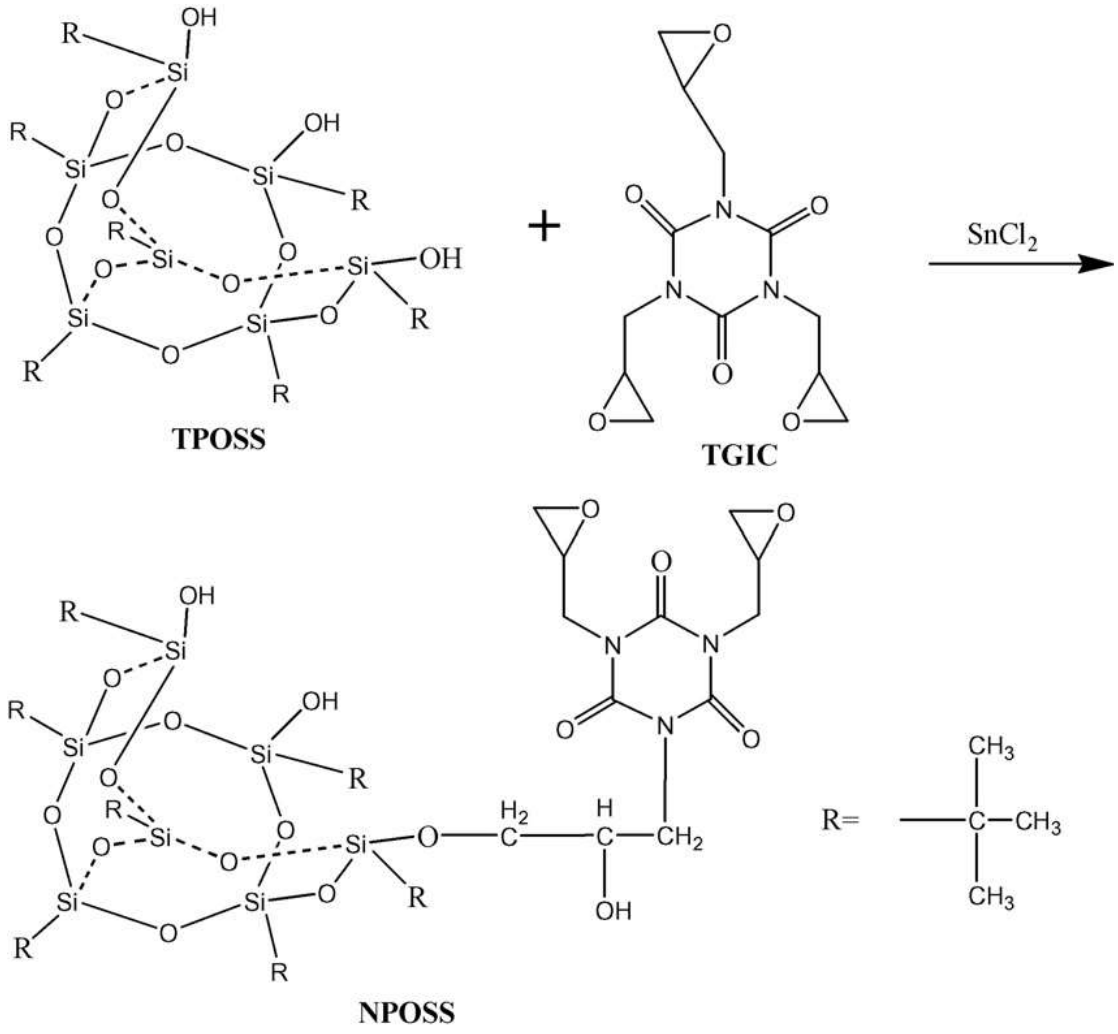

Scheme 1 Reaction between TPOSS and TGIC

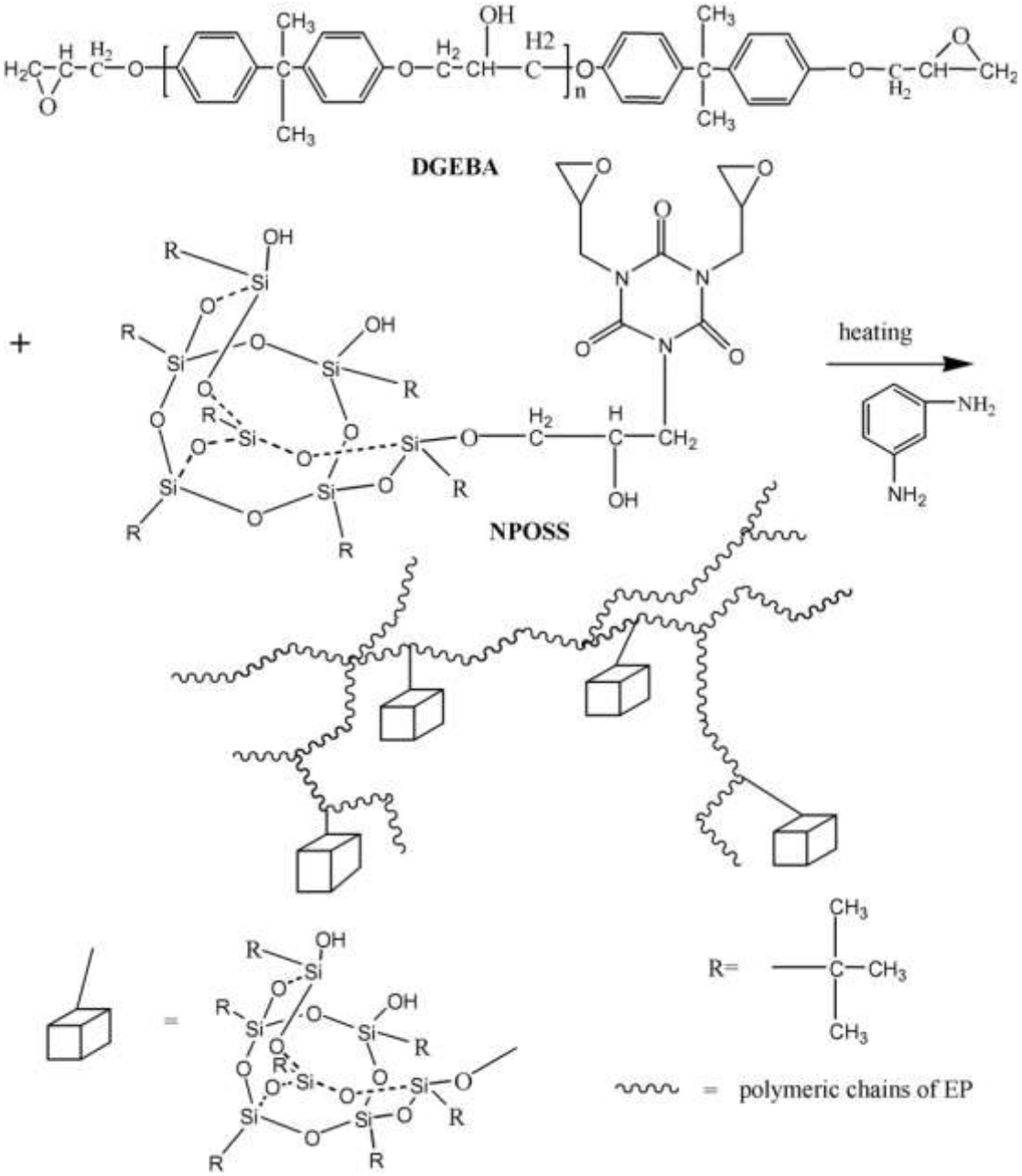

Scheme 2 Reaction process and structure of EP/NPOSS composite

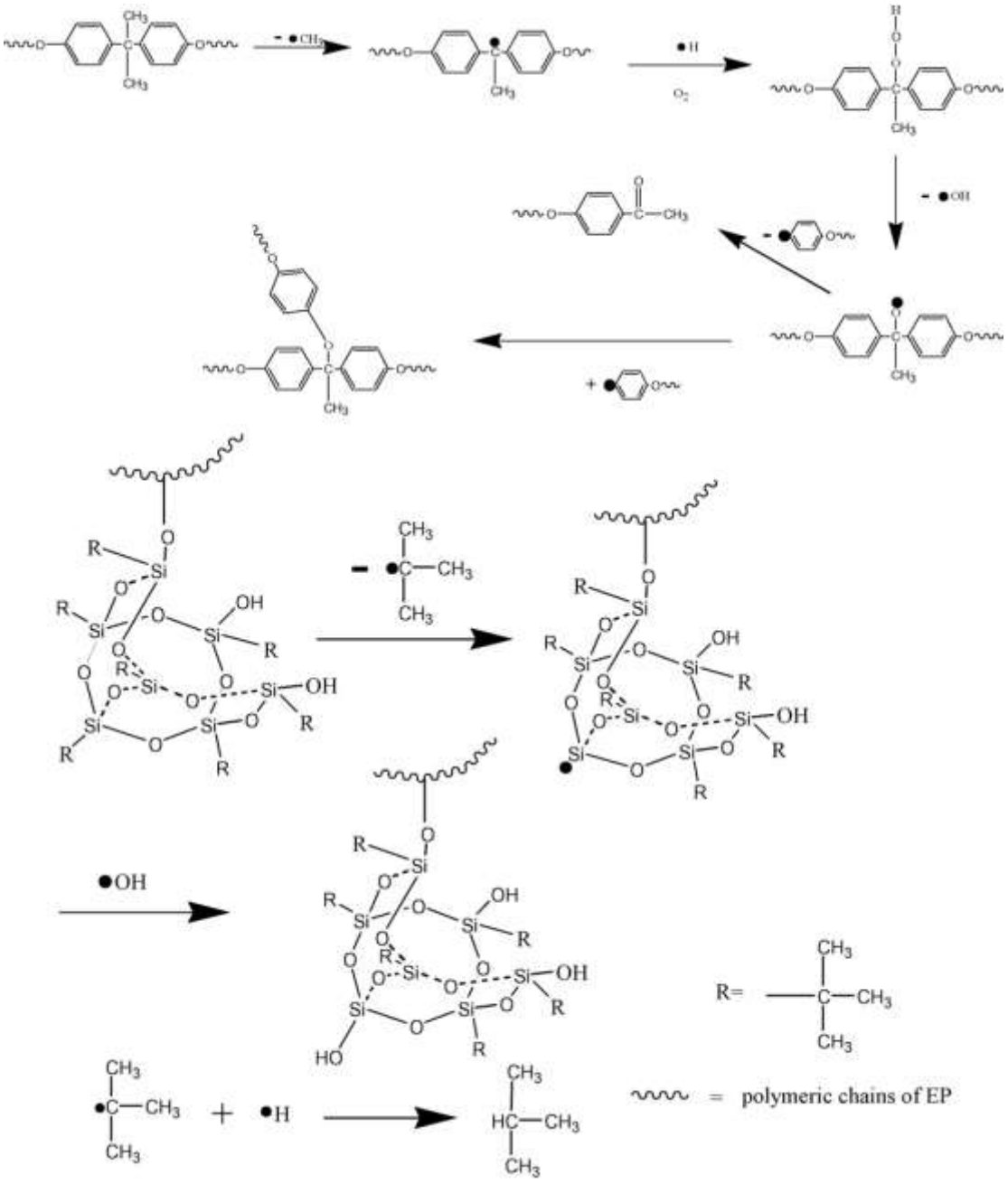

Scheme 3 Proposed mechanism of capture of free radical by NPOSS

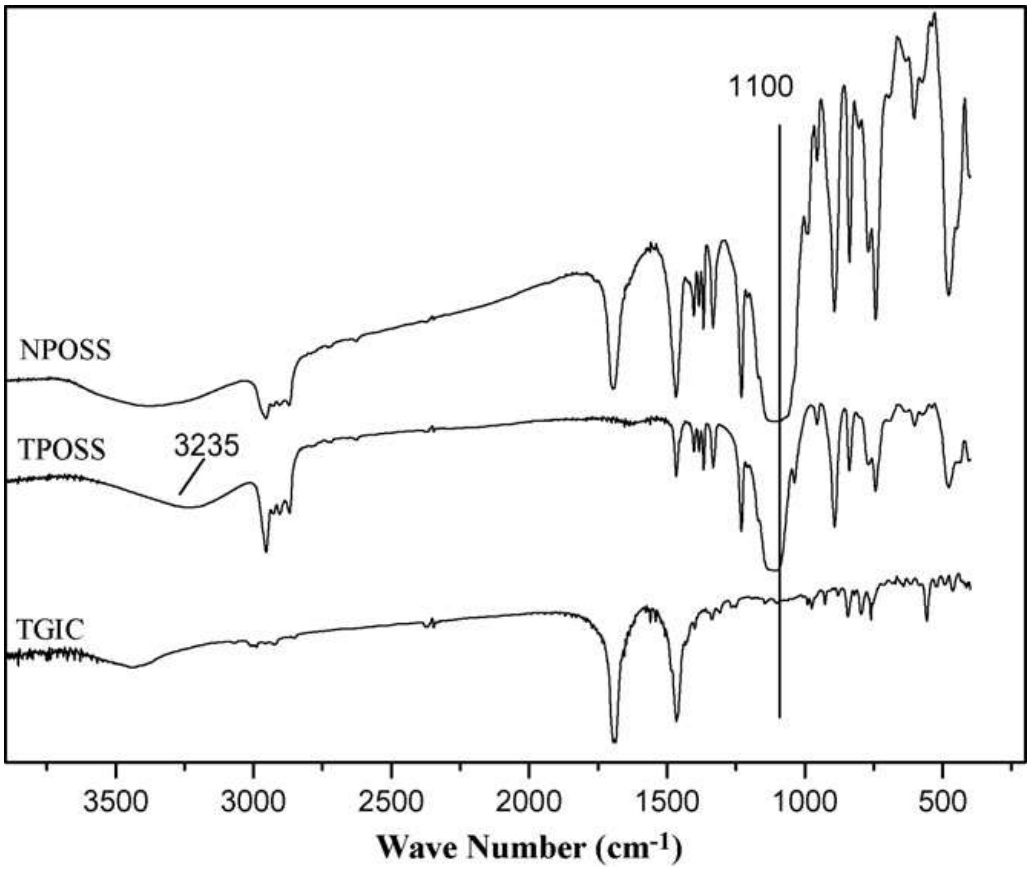

Fig. 1 FTIR spectra of TGIC, TPOSS and NPOSS

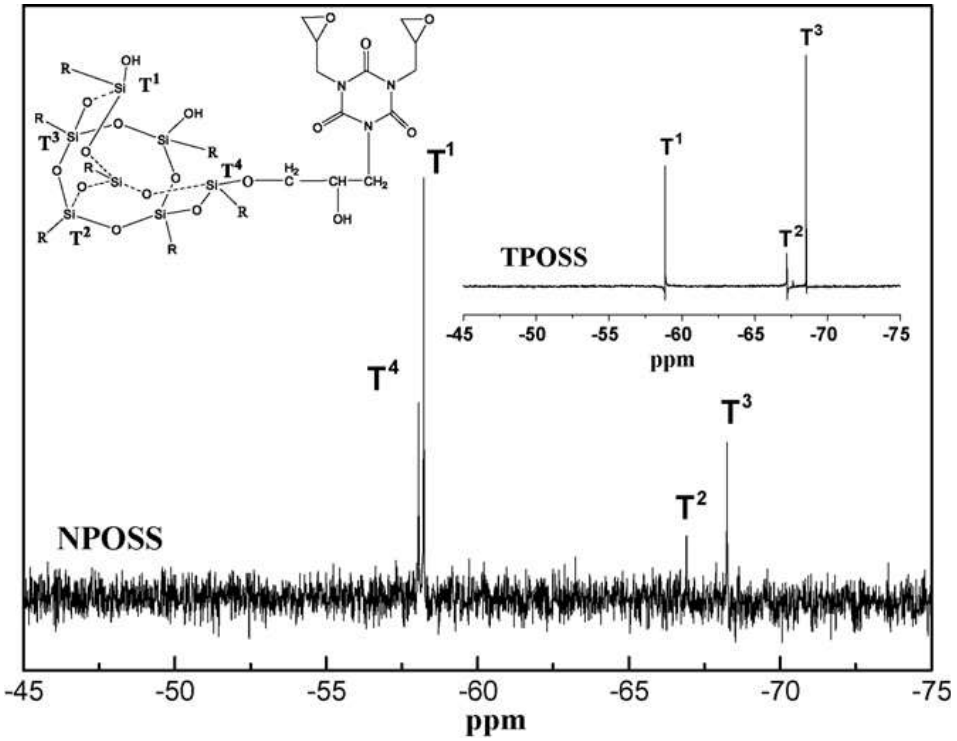

Fig. 2 ^{29}Si NMR spectra of TPOSS and NPOSS

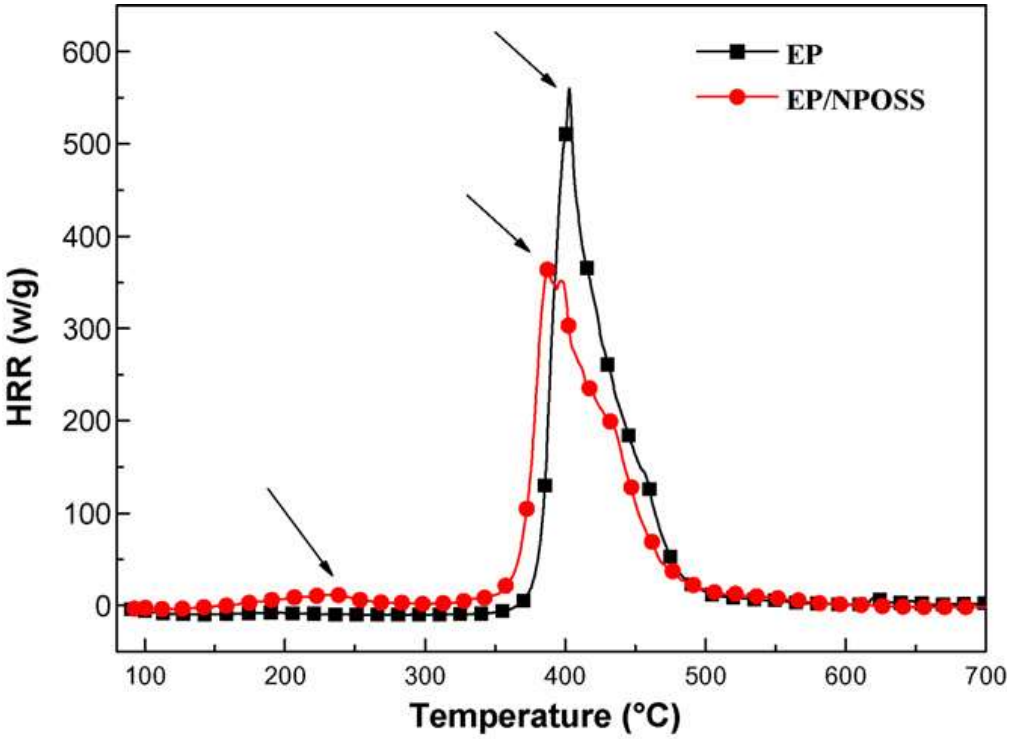

Fig. 3 Heat release rate curves of EP and EP/NPOSS

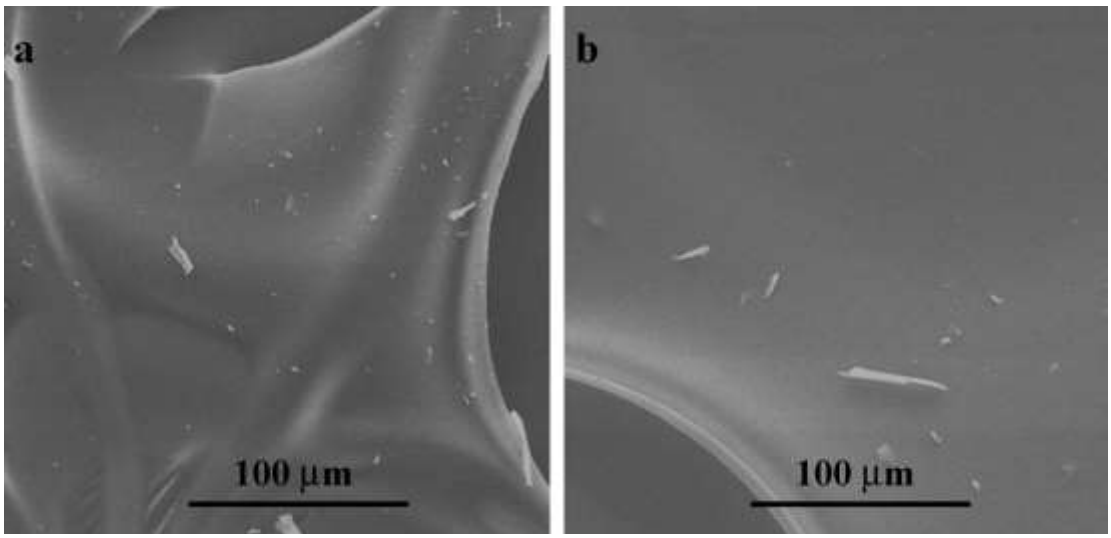

Fig. 4 SEM micrographs of the residual char (× 500): (a) EP; (b) EP/NPOSS

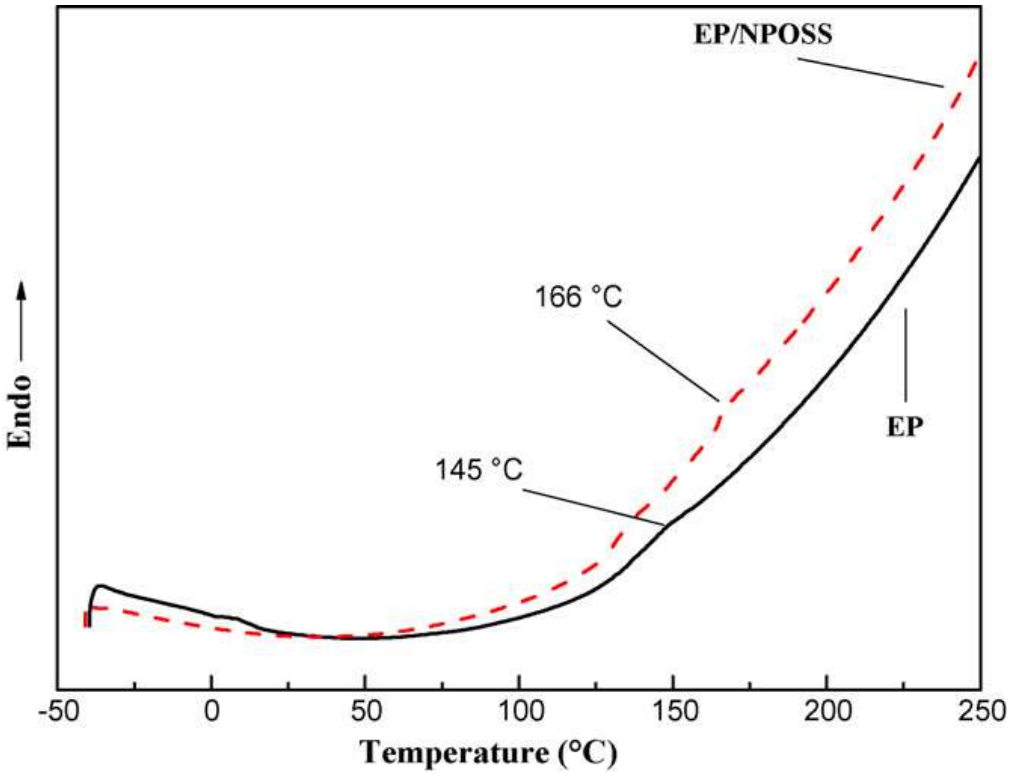

Fig. 5 DSC curves of EP and EP/NPOSS

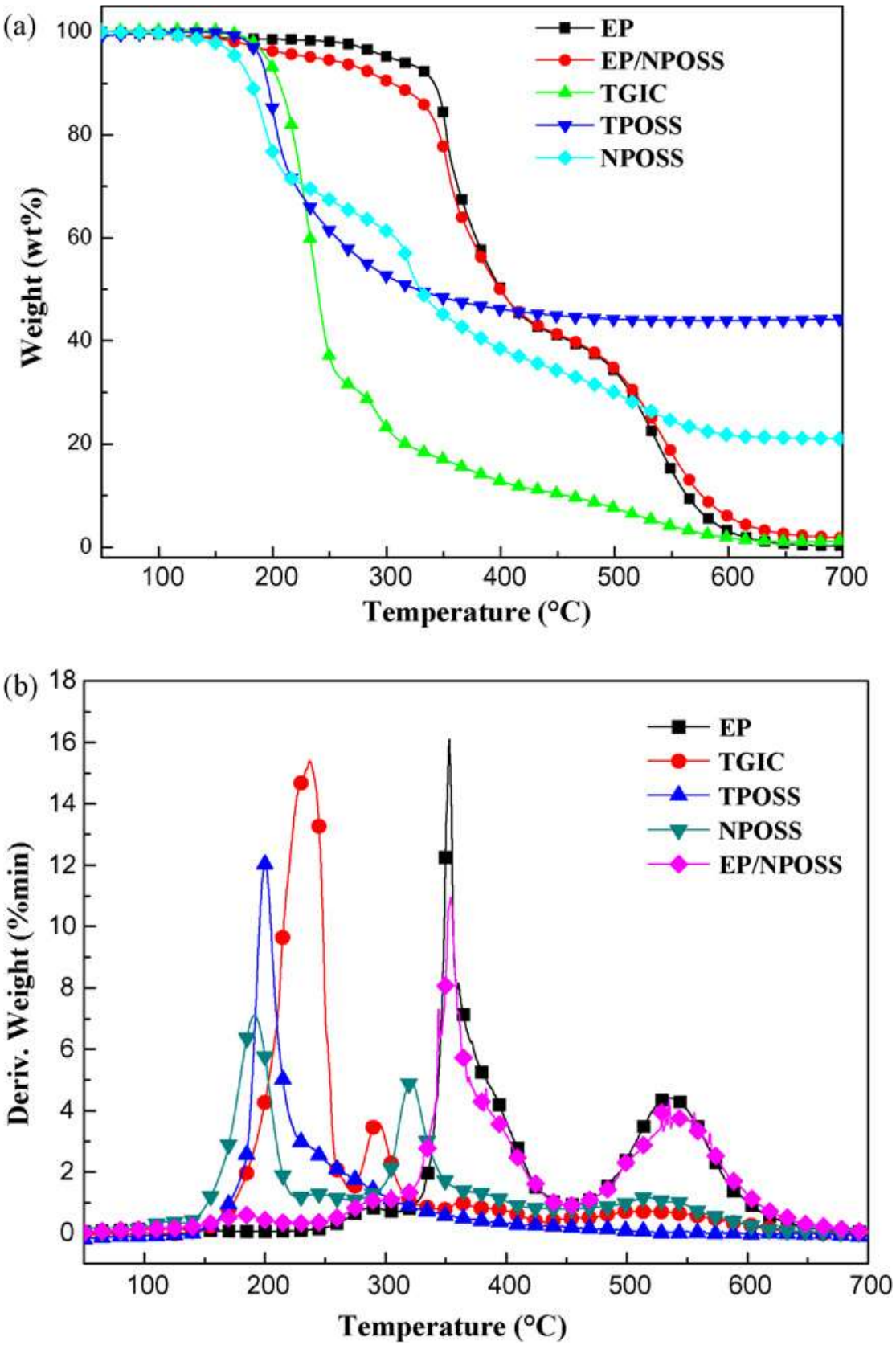

Fig. 6 TG (a) and DTG (b) curves of TGIC, TPOSS, NPOSS, EP and EP/NPOSS under air

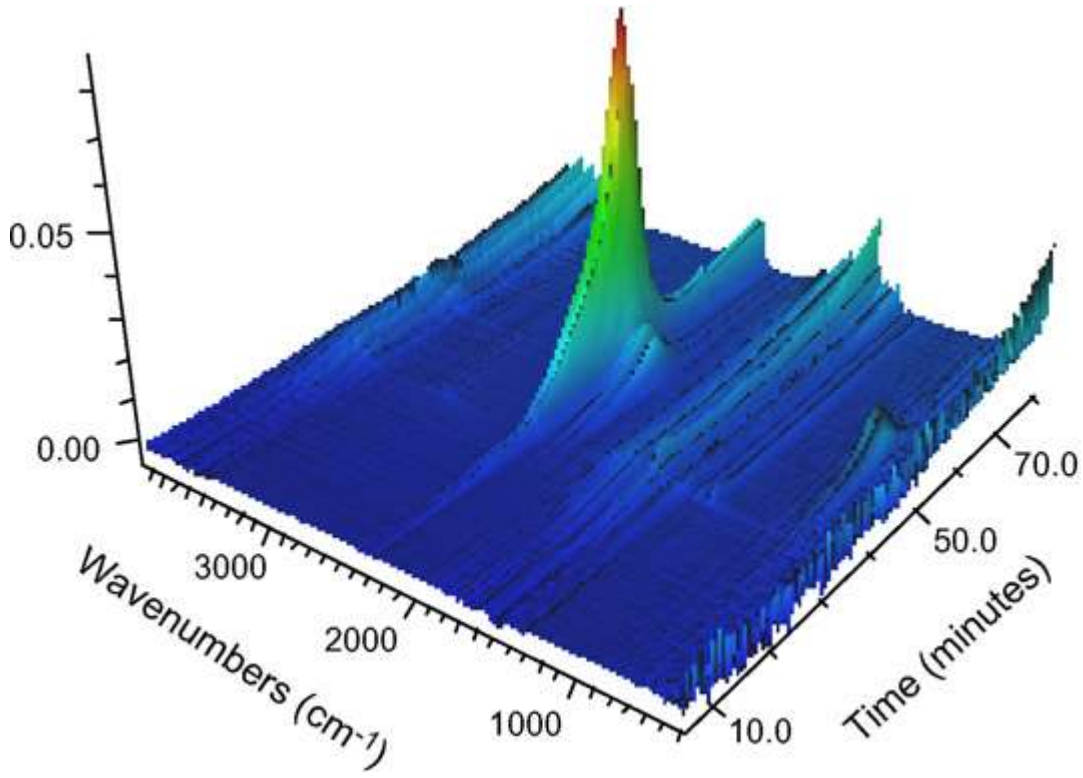

Fig. 7 3D TG-FTIR spectrum of gas phase in the thermal degradation of EP

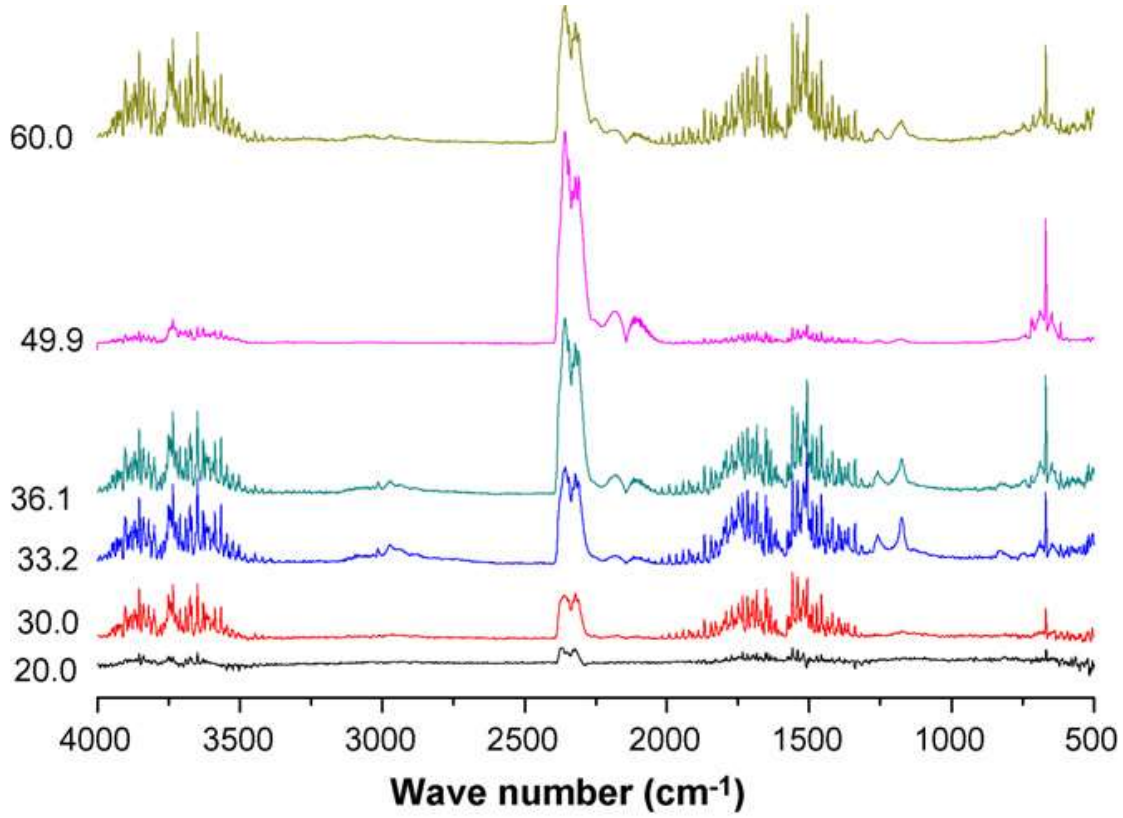

Fig. 8 FTIR spectra of pyrolysis products for EP at different time

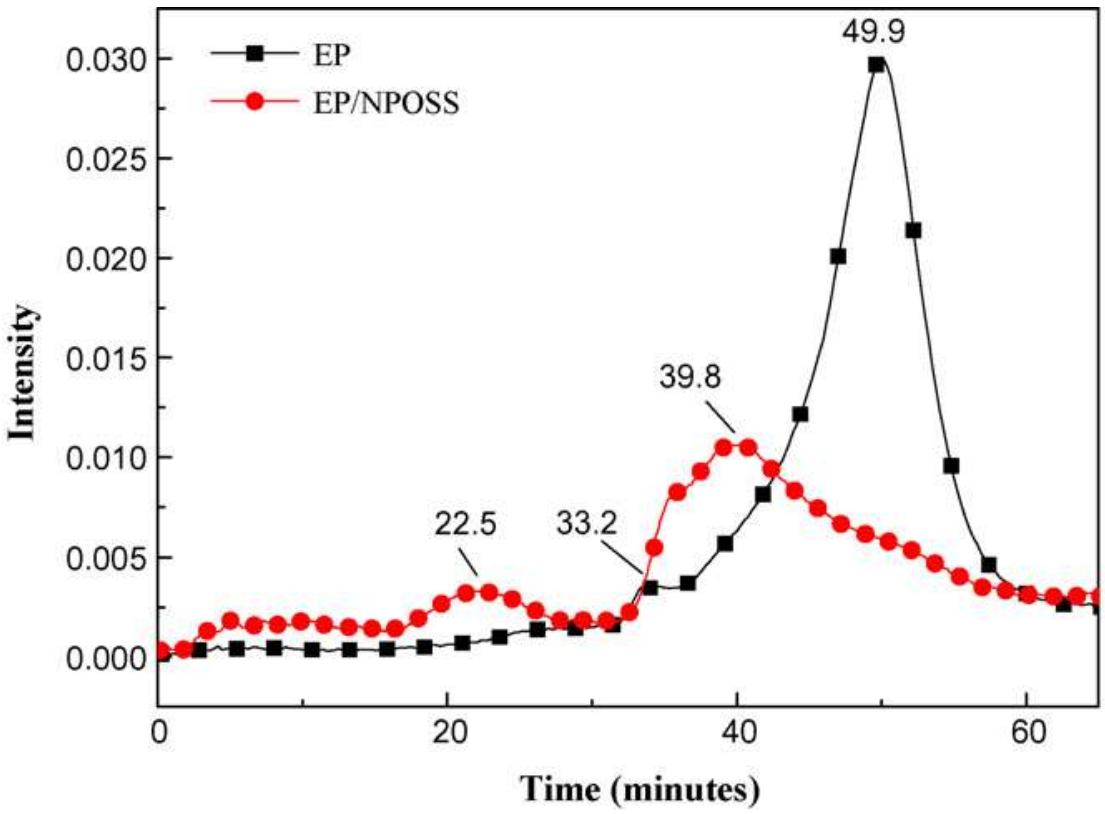

Fig. 9 The intensity of evolved gas products for EP and EP/NPOSS vs. time

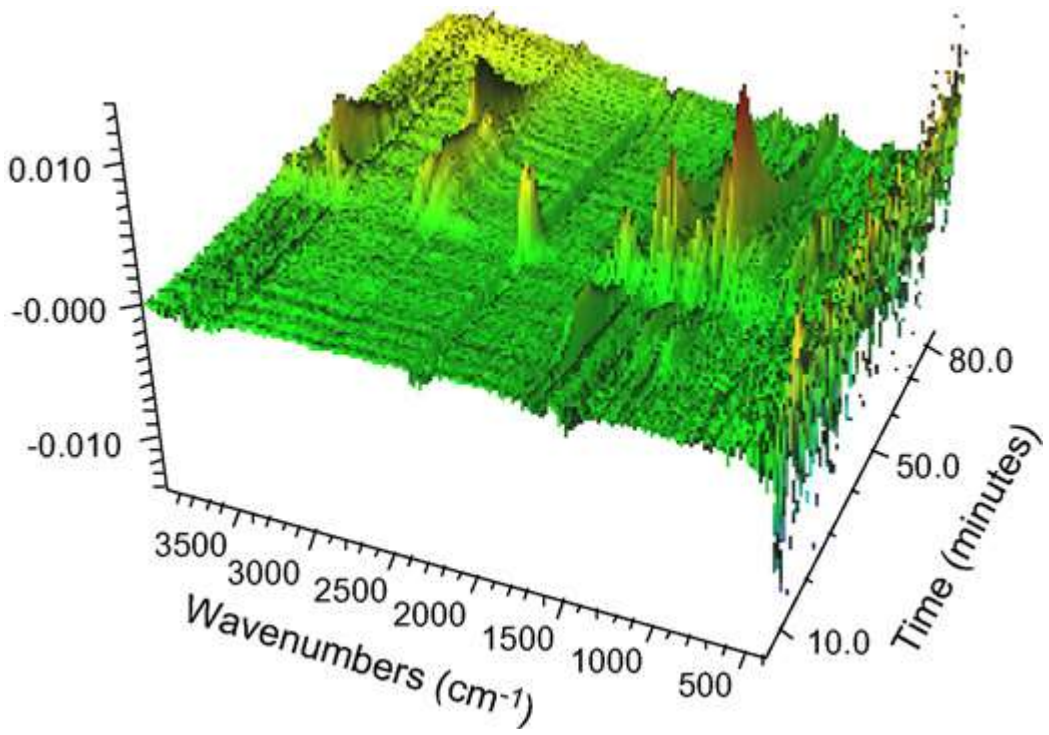

Fig. 10 3D TG-FTIR spectrum of gas phase in the thermal degradation of EP/NPOSS

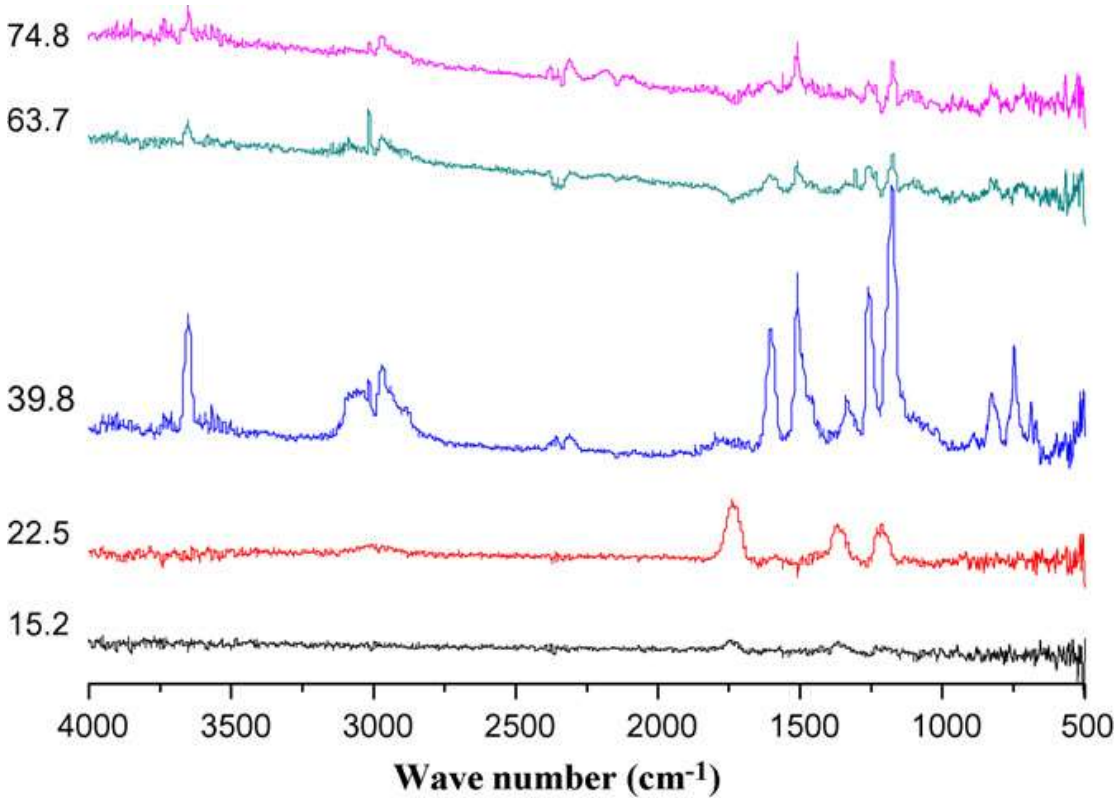

Fig. 11 FTIR spectra of pyrolysis products for EP/NPOSS at different time

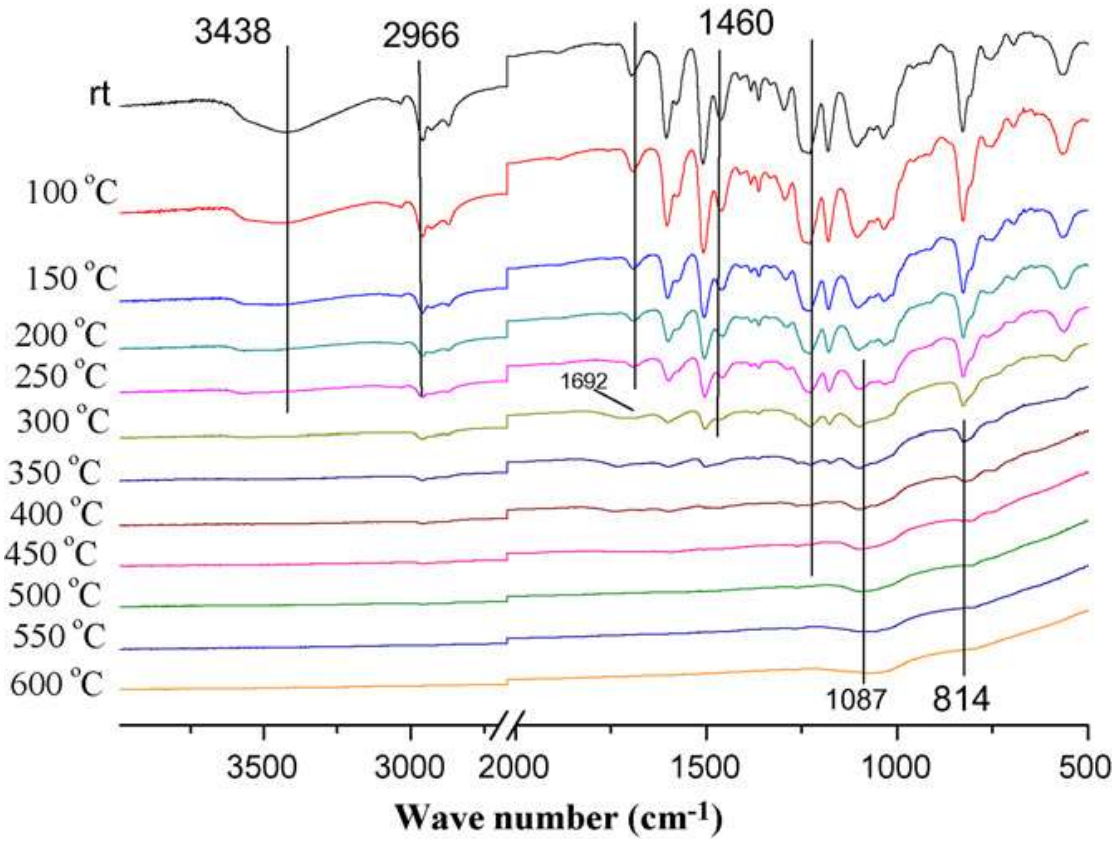

Fig. 12 FTIR spectra of EP/NPOSS at different pyrolysis temperature